AIP | Applied Physics Letters

Sign change in the organic magnetoresistance of tris(8-hydroxyquinolinato)aluminum upon annealing

Hoju Kang, Ik-Jae Lee, and Choon Sup Yoon

Citation: Appl. Phys. Lett. **100**, 073302 (2012); doi: 10.1063/1.3684873

View online: http://dx.doi.org/10.1063/1.3684873

View Table of Contents: http://apl.aip.org/resource/1/APPLAB/v100/i7

Published by the American Institute of Physics.

Sign change in the organic magnetoresistance of tris(8-hydroxyquinolinato)aluminum upon annealing

Hoju Kang,[1] Ik-Jae Lee,[2] and Choon Sup Yoon[1,a)]
[1]*Department of Physics, KAIST, Daejeon 305-701, South Korea*
[2]*Pohang Accelerator Laboratory, Postech, Pohang 790-784, South Korea*

(Received 22 November 2011; accepted 26 January 2012; published online 13 February 2012)

We report the sign change in the magnetoresistance of a tris(8-hydroxyquinolinato)aluminum film with the morphological change from amorphous to crystalline state upon annealing. The negative component of the magnetoresistance followed power law behavior, whereas the positive one showed non-Lorentzian function behavior. The decreasing absolute values of the negative component with increased annealing temperature may be understood by both intersystem-crossing-based mechanism and quenching of triplet excitons. The increasing values of the positive component with increased annealing temperature may be explained by the increase in the hopping probability of charge carriers with increased crystallinity of the film. © *2012 American Institute of Physics*. [doi:10.1063/1.3684873]

Sizable magnetoresistance observed in organic small molecules and π-conjugated polymers at room temperature has attracted a surge of interest in recent years.[1–10] Although intensive efforts have been made in both experiments and theories,[1–8,11–13] a comprehensive understanding of the underlying mechanisms governing these phenomena is yet to come. Several models have been proposed based on hyperfine interactions between polarons and nuclear spins.[9,14–16] In steady state, the intermixing between singlet and triplet polaron pairs occurs through the hyperfine interactions,[17] and an external magnetic field modifies spin configuration of the polaron pairs.[15–17] Recently clear experimental evidence demonstrated that hyperfine interactions played a crucial role in the underlying mechanism of organic magnetoresistance (OMAR).[17,18] OMAR has been shown to be positive and negative, depending on factors, such as the active material,[2,10] device structure,[3,4,19] applied bias voltage,[3,5–7] temperature,[7] and light illumination.[8] OMAR can also be tuned between positive and negative values.[4] Amorphous structures are generally formed in a thin film when organic materials are deposited thermally. In organic semiconductors, the electrical and optical properties of the amorphous structure differ from those of the crystalline one because the disorder can modify intermolecular interactions,[20,21] the statistics of spin states,[22] and the concomitant recombination.[23] The effect of this structural change on OMAR in organic semiconductors, especially on its sign change, is interesting to know. To induce a structural change from a disordered to ordered one, a thin film of tris(8-hydroxyquinolinato)aluminum (Alq_3), which has a simple organic light-emitting diode (OLED) structure, was annealed. Alq_3 was used, because it is thermally stable within a wide temperature range below ~419 °C and different polymorphs can be obtained depending on the annealing temperatue.[21]

In this letter, we report the sign change in OMAR with the morphological change from amorphous to crystalline states; we also discuss the underlying mechanisms associated with the positive and negative OMAR. To investigate the relationship between the sign change in OMAR and the morphology of Alq_3 films, two Alq_3 samples were prepared; one was for magnetoresistance (MR) measurement and the other was for x-ray diffraction (XRD) analysis. Indium tin oxide (ITO) glasses (Geomatec Co. Ltd.) with a sheet resistance of 15 Ω/□ were pre-cleaned and treated with UV-O_3. For the MR measurement, 100 nm-thick Alq_3 (Doosan Electro-Materials Co. Ltd., >99.9%), 1 nm-thick LiF (Cerac Inc.; 99.999%), and 100 nm-thick Al (Cerac Inc., 99.999%) were thermally evaporated in sequence on top of the ITO glasses at a rate of 1 Å/s and a pressure of 10^{-7} Torr (inset of Fig. 1). For the XRD analysis, only 100 nm-thick Alq_3 was evaporated simultaneously with the MR samples on the ITO glasses. Both MR and XRD samples were encapsulated using an UV curable epoxy to protect them from moisture and oxygen. The samples were then respectively annealed at 70, 130, 145, 160, 170, and 180 °C for 1 h at an average

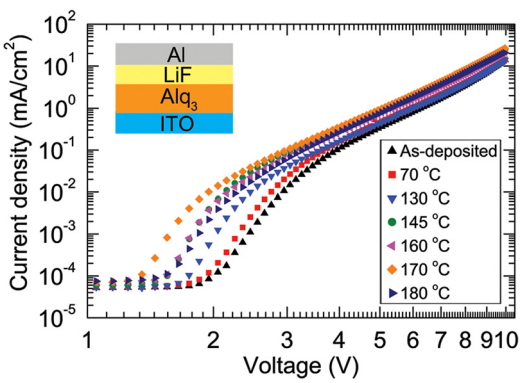

FIG. 1. (Color online) J-V curves of an as-deposited OLED device (up-pointing triangle) as well as devices annealed at 70 (square), 130 (down-pointing triangle), 145 (circle), 160 (left-pointing triangle), 170 (diamond), and 180 °C (right-pointing triangle). Inset: a schematic diagram of the OLED device structure.

a)Author to whom correspondence should be addressed. Electronic mail: csyoon@kaist.ac.kr. Tel.: +82 42 350 2532. Fax: +82 42 350 8780.

temperature lowering rate of 0.6 °C/min in a dry oven. *J-V* curves were obtained to evaluate the characteristics of the OLED device using a sourcemeter (Keithley 2400) at room temperature. The current drift during the OMAR measurement was compensated for by the method used in the previous work of the authors.[24] The MR sample was placed between the poles of an electromagnet such that the direction of the current was perpendicular to the magnetic field, which ranged from 0 to 260 mT. For the XRD analysis, a thin film x-ray diffractometer (Rigaku, 12 kW) with monochromatic Cu K_α radiation was used.

The *J-V* curves of the as-deposited and annealed OLED devices are shown in Fig. 1. The OLED device annealed at 70 °C did not show any significant difference from the as-deposited one. However, remarkably increased currents were observed at low bias voltages when the devices were annealed above 130 °C. The drop in the currents of the sample annealed at 180 °C may be ascribed to the partial damage of the aluminum cathode due to the structural change in the Alq_3 film by crystallization. However, the diode characteristics remained in the annealed devices as long as the annealing temperatures were kept below 190 °C. The diode characteristics disappeared at an annealing temperatures of 190 °C and above, and the MR could not be measured either.

Figure 2 shows the fluorescence optical micrographs of the Alq_3 films annealed at different temperatures up to 190 °C. The as-deposited Alq_3 film [Fig. 2(a)] as well as the films annealed at 70 and 130 °C [Figs. 2(b) and 2(c), respectively] showed uniform contrast, indicating the amorphous structure of the films. When the Alq_3 film was annealed at 145 °C, anomalies that were about 1 μm in size, with triangular and square shapes, appeared in the fluorescence image [Fig. 2(d)]. From these anomalies, needle-shaped crystals started to grow at an annealing temperature of 160 °C, as shown in Fig. 2(e). The area occupied by the crystals became larger with increased annealing temperatures [Figs. 2(f) and 2(g)], and most of the area was covered by needle-shaped crystals at an annealing temperature of 190 °C [Fig. 2(h)]. The glass transition temperature of a 56 nm-thick Alq_3 film was reported to be about 130 °C,[25] which explained why the film remained amorphous at an annealing temperature of 130 °C and below.

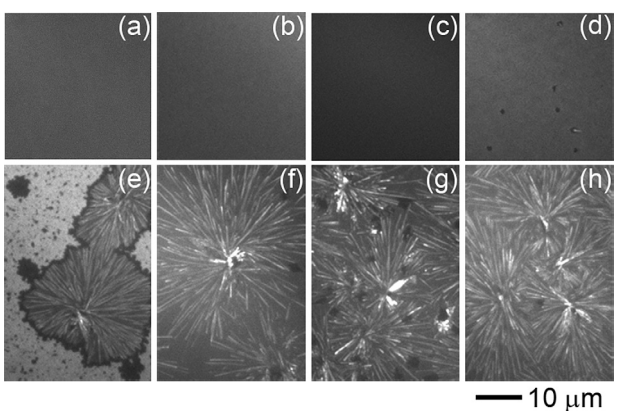

FIG. 2. UV fluorescence optical microscope images of (a) an as-deposited film, as well as films annealed at (b) 70, (c) 130, (d) 145, (e) 160, (f) 170, (g) 180, and (h) 190 °C. The scale bar indicates 10 μm.

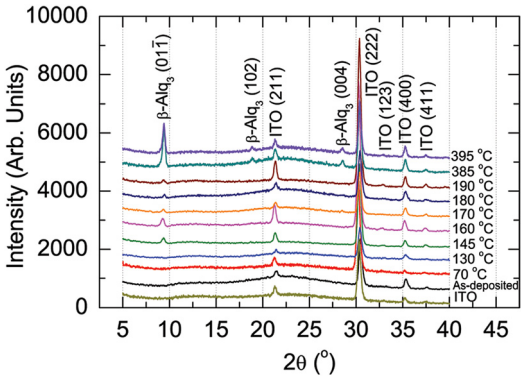

FIG. 3. (Color online) X-ray diffraction spectra of an ITO substrate, an as-deposited film of Alq_3, and the Alq_3 films annealed at different temperatures.

The morphology of the Alq_3 film was examined by the XRD analysis. Figure 3 shows the XRD spectra of the as-deposited and annealed Alq_3 films. The peaks at $2\theta = 21.3°$, 30.4°, 35.28°, and 37.49° corresponded to the reflections from the (211), (222), (400), and (411) planes of the ITO substrate. On the other hand, The peaks at $2\theta = 9.38°$, 18.83°, and 28.78° came from the $(01\bar{1})$, (102), and (004) planes of the β-phase of Alq_3, respectively.[26] The as-deposited Alq_3 film and the films annealed at 70 and 130 °C did not show any diffraction peak of Alq_3, which indicated the amorphous structure of the Alq_3 films. However, the films annealed at 145, 160, 170, 180 and 190 °C showed diffraction peaks at $2\theta = 9.38°$, indicating the crystalline β-phase. These findings well agreed with the fluorescence optical microscope images in Figs. 2(d)–2(h). At annealing temperatures of 385 and 395 °C, additional diffraction peaks for the β-phase of Alq_3 appeared at $2\theta = 18.83°$ and 28.78°, which were reflected from the (102) and (004) planes, respectively.

All MR measurements were conducted at a constant bias voltage of 7 V. The MR values, $\Delta R(B)/R(0) = [R(B)-R(0)]/R(0)$, of the as-deposited OLED devices and those annealed at different temperatures between 70 and 180 °C are shown in Fig. 4(a). The MR for the device annealed at 190 °C could not be measured because the magnetic current signal was severely deteriorated. This deterioration may be caused by the damage to the aluminum electrode by the needle-shaped Alq_3 microcrystals grown in the direction normal to the plane of the film.

As shown in Fig. 4(a), all MR values of the as-deposited Alq_3 film and those annealed at 70 and 130 °C were negative in the range of 0 to 260 mT. On the other hand, all MR values were positive for the devices annealed at 170 and 180 °C in the same range of magnetic field. For the devices annealed at 145 and 160 °C, the MR values initially increased with the positive values, reached the maximum, and then decreased, changing the sign from positive to negative at 48 and 125 mT, respectively. To understand the MR mechanism, the observed MR values in Fig. 4(a) may be decomposed into two parts: positive and negative values as $MR(B) = MR^+(B) + MR^-(B)$. The negative MR values (MR^-) showed a power law behavior toward the magnetic field B^n [Fig. 4(b)], whereas the positive MR values (MR^+) showed non-Lorentzian function behavior

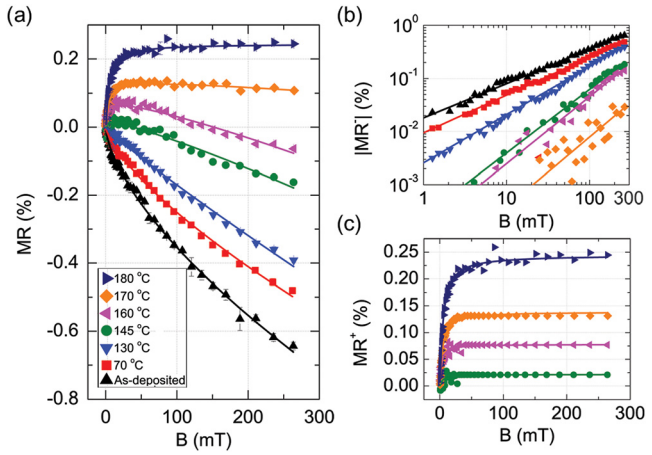

FIG. 4. (Color online) (a) MR vs. B for an as-deposited Alq_3 film (up-pointing triangle) as well as films annealed at 70 (square), 130 (down-pointing triangle), 145 (circle), 160 (left-pointing triangle), 170 (diamond), and 180 °C (right-pointing triangle). (b) Absolute value of the negative component of the magnetoresistance in a log-log scale, and (c) positive component of the magnetoresistance in a linear scale. The solid lines are fitted curves.

[Fig. 4(c)]. The MR^- component appeared in the as-deposited film and those annealed at all temperatures except 180 °C. With increased annealing temperature, the absolute values of MR^- decreased, and the exponent n increased from 0.65 for the as-deposited film to 1.32 for the film annealed at 170 °C. In comparison, MR^+ appeared only in the films annealed at and above 145 °C, suggesting the link between the MR^+ in the present study and the ordering of Alq_3 molecules in the β-phase crystalline structure.

The as-deposited Alq_3 film showed an amorphous structure, in which the positions and orientations of Alq_3 molecules were in a disordered manner. The intrinsic polymorphism and local fluctuations in the enantiomeric concentrations during evaporation, combined with the strong dipole-dipole interactions between Alq_3 molecules,[20] are responsible for the amorphous nature of the sublimed thin films.[26] In the current work, at annealing temperatures of 145 °C and above, the area of the crystalline region increased with increased annealing temperature, as shown in Fig. 2. In the crystalline β-phase, an Alq_3 molecule was linked to one neighboring Alq_3 molecule by π-π interactions that occurred between a pair of neighboring parallel hydroxyquinoline ligands lying in the $[\bar{3}21]$ direction, and to the other neighboring molecule by π-π interactions between a pair of neighboring parallel hydroxyquinoline ligands lying in the $[0\bar{1}1]$ direction.[26] Such π-π overlap interactions provided an extended one-dimensional channel facilitating charge carrier hopping along the crystallographic c-axis, whereas no such channel existed in the amorphous structure. As annealing temperature increased, the packing density of Alq_3 molecules also increased not only in the amorphous films but also in the crystalline ones,[26,27] leading to decreasing average intermolecular distance.

The decreasing absolute values of MR^- with increased annealing temperature in Fig. 4(b) may be understood by the intersystem crossing (ISC)-based mechanism based on hyperfine interactions.[14–17,28] The ISC occurs mainly in polaron pairs and is affected by both external magnetic field and charge separation distance.[15,16,28,29] The ratio of singlet to triplet polaron pairs is larger in the presence of an external magnetic field than that with zero field. This is because the transition from singlet to triplet polaron pairs with $\Delta m = 0$ only is allowed after the degeneracy of the triplet state is removed by the Zeeman splitting. Since singlet polaron pairs, in general, have larger dissociation rate than triplet ones,[1,15] more secondary charges are generated in the magnetic field, leading to a negative magnetoresistance. As the intermolecular distance decreases upon annealing, the ISC from a singlet to a triplet state is diminished by the increased energy difference between the two states due to stronger exchange interaction.[14–16] If an external magnetic field is applied, the ISC will be further suppressed. As a consequence, the ratio of the number of singlet polaron pairs increased by the magnetic field to the number of singlet polaron pairs in the zero field can decrease as the intermolecular distance shortens, which results in the decrease in the magnitude of MR^- with increased annealing temperature [Fig. 4(b)].

The fact that the MR^+ component appeared only in the films annealed at and above 145 °C suggests that MR^+ may be related to the crystalline nature of Alq_3 films. The major differences between the amorphous and crystalline structures are positional and orientational orderings and a higher packing density[26,27] in the crystalline phase. The effect of higher packing density resulted in the shorter average intermolecular distance, which was discussed in association with the ISC-based mechanism. The positional and orientational orderings in the β-phase of Alq_3 films provided extended one-dimensional channels for charge carriers hopping along the crystallographic c-axis.[26] Therefore, it is reasonable to expect that an efficient hopping transport through the channels may bring about the appearance of MR^+ component by the charge carriers such as polarons. When the hopping charges are captured, the same-sign polaron-pairs favor singlet states than triplet states to comply with the Pauli principle. In the presence of an external magnetic field, the probability of forming same-sign polaron-pairs becomes reduced because of increased spin order, leading to a positive magnetoresistance. As the area of crystalline region in Alq_3 films increases with increased annealing temperature, the hopping probability of the charge carriers also increases. Therefore, the higher the annealing temperatures of the Alq_3 films, the larger the effect of the magnetic field on the charge-capture. This is reflected in Fig. 4(c), which shows larger magnitude of MR^+ with higher annealing temperatures. The observed MR^+ can be fitted to an empirical non-Lorentzian function $B^2/(B_0 + B)^2$, as predicted by the capture-based mechanism,[5,9,28] with $B_0 = 0.944$, 1.106, 1.826, and 2.205 mT for the annealing temperatures of 145, 160, 170, and 180 °C, respectively.

The triplet excitons have a much longer life time and larger population than singlet excitons, so they can affect injection current through interactions with (i) other triplet excitons[30] and (ii) charge carriers.[31] The process (i) is called triplet-triplet annihilation (TTA), in which a triplet exciton pair can annihilate to yield a singlet excited state and a singlet ground state.[30] TTA generally enhances electroluminescence in organic light emitting diodes through the delayed fluorescence. It also possibly affects the injection current if

the singlet exciton dissociates into free charges. An external magnetic field ranging from 10 to 100 mT can substantially reduce the ISC rate from singlet to triplet polaron pairs, leading to a decrease in the concentration of the triplet polaron pairs and consequently triplet excitons.[1,4,32] As TTA is proportional to the density square of triplet excitons, the concentration of singlet excitons produced from the TTA can be diminished in the presence of an external magnetic field, leading to MR^+. The probability of forming a triplet exciton pair can increase as the intermolecular distance of Alq_3 decreases with increased annealing temperature. This result leads to an increase in the magnitude of MR^+ with increased annealing temperature. The MR^+ caused by the TTA is expected to appear in Alq_3 films annealed at all temperatures because the packing density of Alq_3 molecules increases with increased annealing temperature both in amorphous and crystalline films.[26,27] Considering that TTA has a high field effect,[32] it cannot alone explain the sign change in MR for the films annealed at 145 °C at 48 mT [Fig. 4(a)]. However, the TTA effect may superpose on the effect caused by the ICS- and capture-based mechanisms. Even in this case, the magnitude of MR^+ due to the TTA can be negligibly small compared with that caused by both mechanisms, because the dissociation rate of singlet excitons is much smaller than that of singlet polaron pairs. Other experimental evidence, which supports this view, indicates that TTA does not influence the magnetocurrent,[33] and the delayed fluorescence from TTA is hardly observed at room temperature[34] in Alq_3.

The process (ii) can increase injection current by dissociating a triplet exciton into an electron and a hole[4] or decrease injection current through quenching of triplet excitons.[14] As an external magnetic field can decrease the concentration of the triplet polaron pairs and consequently the triplet excitons,[32] the dissociation and quenching of the triplet excitons lead to MR^+ and MR^-, respectively. Considering that all MR values for the as-deposited film are negative [Fig. 4(a)], the process involving the dissociation of the triplet excitons alone cannot explain the experimental result. The quenching of triplet excitons, however, gives the similar effect on MR to the dissociation of singlet polarons in the ISC, and therefore both effects on the MR^- in Fig. 4(b) cannot be distinguished.

A similar annealing effect on MR has been reported in amorphous silicon[35,36] and germanium.[36] However, the exponent in the power law of MR^- was found to be independent of the annealing temperature. This might be attributed to the almost instantaneous occurrence of crystallization in the entire areas of the Si and Ge films at a critical temperature, because the atoms are bonded by strong covalent bonds. Meanwhile, crystallization in the entire area of the Alq_3 films in the current study did not occur instantaneously but occurred rather successively with increased annealing temperature, because weak van der Waals interactions are responsible for the bonding of the molecules and the annealing time was 1 h.

In summary, we presented the sign change in the magnetoresistance of Alq_3 films upon annealing. MR^- appeared in the as-deposited film and those annealed at all temperatures except 180 °C, whereas MR^+ appeared only in the films annealed at and above 145 °C. The MR^- and MR^+ followed a power law behavior and non-Lorentzian function behavior, respectively. The magnitude variations of MR^- and MR^+ as a function of annealing temperature were explained by existing models of OMAR.

This work was supported by the Information Technology R&D Program of Ministry of Knowledge Economy (2008-F024-01).

[1]J. Kalinowski, M. Cocchi, D. Virgili, P. Di Marco, and V. Fattori, Chem. Phys. Lett. **380**, 710 (2003).
[2]Ö. Mermer, G. Veeraraghavan, T. L. Francis, Y. Sheng, D. T. Nguyen, M. Wohlgenannt, A. Khler, M. K. Al-Suti, and M. S. Khan, Phys. Rev. B **72**, 205202 (2005).
[3]P. Desai, P. Shakya, T. Kreouzis, and W. P. Gillin, J. Appl. Phys. **102**, 073710 (2007).
[4]B. Hu and Y. Wu, Nat. Mater. **6**, 985 (2007).
[5]F. L. Bloom, W. Wagemans, M. Kemerink, and B. Koopmans, Phys. Rev. Lett. **99**, 257201 (2007).
[6]F. J. Wang, H. Bässler, and Z. V. Vardeny, Phys. Rev. Lett. **101**, 236805 (2003).
[7]J. D. Bergeson, V. Prigodin, D. M. Lincoln, and A. Epstein, Phys. Rev. Lett. **100**, 067201 (2008).
[8]Y. L. Lei, Q. L. Song, Y. Zhang, P. Chen, R Liu, Q. M. Zhang, and Z. H. Xiong, Org. Electron. **10**, 1288 (2009).
[9]P. A. Bobbert, T. D. Nguyen, F. W. A. van Oost, B. Koopmans, and M. Wohlgenannt, Phys. Rev. Lett. **99**, 216801 (2007).
[10]Z. Xu and B. Hu, Adv. Funct. Mater. **18**, 2611 (2008).
[11]A. I. Shushin, Phys. Rev. B **84**, 115212 (2011).
[12]S. P. Kersten, A. J. Schellenkens, B. Koopmans, and P. A. Bobbert, Phys. Rev. Lett. **106**, 197402 (2011).
[13]D. R. McCamey, K. J. van Schooten, W. J. Baker, S.-Y. Lee, S.-Y. Paik, J. M. Lupton, and C. Boehme, Phys. Rev. Lett. **104**, 017601 (2010).
[14]P. Desai, P. Shakya, T. Kreouzis, W. P. Gillin, N. A. Morley, and M. R. J. Gibbs, Phys. Rev. B **75**, 094423 (2007).
[15]Y. Wu, Z. Xu, and B. Hu, Phys. Rev. B **75**, 035214 (2007).
[16]V. N. Prigodin, J. D. Bergeson, D. M. Lincoln, and A. J. Epstein, Synth. Met. **156**, 757 (2006).
[17]T. D. Nguyen, B. R. Gautam, E. Ehrenfreund, and Z. V. Vardeny, Phys. Rev. Lett. **105**, 166804 (2010).
[18]T. D. Nguyen, G. Hukic-Markosian, F. Wang, L. Wojcik, X.-G. Li, E. Ehrenfreund, and Z. V. Vardeny, Nat. Mater. **9**, 345 (2010).
[19]C. Gärditz and A. G. Muckl, J. Appl. Phys. **98**, 104507 (2005).
[20]S.-J. Kim and T. E. Karis, J. Mater. Res. **10**, 2128 (1995).
[21]M. Cölle, J. Gmeiner, W. Milius, H. Hillebrecht, and W. Brutting, Adv. Funct. Mater. **13**, 108 (2003).
[22]S. P. Kersten, A. H. Schellekens, B. Koopmans, and P. A. Bobbert, Synth. Met. **161**, 613 (2011).
[23]R. A. Street, Phys. Rev. B **84**, 075208 (2011).
[24]H. Kang, C. H. Park, J. Lim, C. Lee, W. Kang, and C. S. Yoon, "Power law behavior of magnetoresistance in tris(8-hydroxyquinolinato)aluminum-based organic light-emitting diodes" (unpublished).
[25]M. S. Xu and J. B. Xu, Thin Solid Films **491**, 317 (2005).
[26]M. Brinkmann, G. Gadret, M. Muccini, C. Taliani, N. Masciocchi, and A. Sironi, J. Am. Chem. Soc. **122**, 5147 (2000).
[27]G. G. Malliaras, Y. Shen, D. H. Dunlap, H. Murata, and Z. H. Kafafi, Appl. Phys. Lett. **79**, 2582 (2001).
[28]M. Shao, Y. Dai, D. Ma, and B. Hu, Appl. Phys. Lett. **99**, 073302 (2011).
[29]S. Majumdar, H. S. Majumdar, H. Aarnio, D. Vanderzande, R. Laiho, and R. Österbacka, Phys. Rev. B **79**, 201202(R) (2009).
[30]R. C. Johnson and R. E. Merrifield, Phys. Rev. B **1**, 896 (1970).
[31]W. Helfrich and W. G. Schneidere, Phys. Rev. Lett. **14**, 229 (1965).
[32]Y. Zhang, R. Liu, Y. L. Lei, and Z. H. Xiong, Appl. Phys. Lett. **94**, 083307 (2009).
[33]Y. L. Lei, Y. Zhang, R. Liu, P. Chen, Q. L. Song, and X. H. Xiong, Org. Electron. **10**, 889 (2009).
[34]M. Cölle and C. Gärditz, Appl. Phys. Lett. **84**, 3160 (2004).
[35]R. M. Mehra, S. C. Agarwal, S. Rani, R. Shyam, and P. C. Mathur, Thin Solid Films **76**, 379 (1981).
[36]R. M. Mehra, R. Shyam, and P. C. Mathur, Thin Solid Films **100**, 81 (1983).